Pilot Design Schemes for Sparse Channel Estimation in OFDM Systems

Chenhao Qi, *Member, IEEE*, Guosen Yue, *Senior Member, IEEE*, Lenan Wu, Yongming Huang, *Member, IEEE*, and Arumugam Nallanathan, *Senior Member, IEEE*

***Abstract*—In this paper, we consider the pilot design based on the mutual incoherence property (MIP) for sparse channel estimation in orthogonal frequency-division multiplexing (OFDM) systems. With respect to the length of channel impulse response (CIR), we first derive a sufficient condition for the optimal pilot pattern generated from the cyclic different set (CDS). Since the CDS does not exist for most practical OFDM systems, we propose three pilot design schemes to obtain a near-optimal pilot pattern. The first two schemes, including stochastic sequential search (SSS) and stochastic parallel search (SPS), are based on the stochastic search. The third scheme called iterative group shrinkage (IGS) employs a tree-based searching structure and removes rows in a group instead of removing a single row at each step. We later extend our work to multiple-input–multiple-output (MIMO) systems and propose two schemes, i.e., sequential design scheme and joint design scheme. We also combine them to design the multiple orthogonal pilot patterns, i.e., using the sequential scheme for the first several transmit antennas and using the joint scheme to design the pilot pattern for the remaining transmit antennas. Simulation results show that the proposed SSS, SPS, and IGS converge much faster than the cross-entropy optimization and the exhaustive search and are thus more efficient. Moreover, SSS and SPS outperform IGS in terms of channel estimation performance.**

***Index Terms*—Compressed sensing (CS), massive multiple-input–multiple-output (MIMO), pilot design, sparse channel estimation.**

I. Introduction

RECENT advances in compressed sensing (CS) have demonstrated that the application of sparse recovery to channel estimation, i.e., sparse channel estimation, can be more efficient than the conventional channel estimation approaches due to the sparse nature of multipath wireless channels [1], [2]. The CS techniques for pilot-assisted channel estimation have been widely investigated [3]–[5], and many sparse recovery algorithms have been applied for channel estimation, e.g., orthogonal matching pursuit (OMP), compressive sampling matching pursuit, and basis pursuit. Another focus of the sparse channel estimation is the design of pilots. According to the restricted isometry property (RIP) [6], it has been shown that the measurement using random matrices guarantees a high probability of sparse recovery, indicating that the randomly generated pilot pattern is statistically optimal. However, the implementation of the random pilot pattern is more challenging in practical systems due to its high complexity, large storage, and low efficiency. To the best of authors' knowledge, most commercial orthogonal frequency-division multiplexing (OFDM) systems employ a deterministic pilot pattern, which allocates a time–frequency unit for each pilot symbol and keeps it unchanged during the data transmission. Therefore, in this paper, we focus on the deterministic pilot design for sparse channel estimation in OFDM systems. In [7] and [8], it has been shown that the pilot pattern generated from the cyclic different set (CDS) is optimal, and in [9], we have proposed an iterative tree-based searching algorithm to obtain a deterministic pilot pattern. In [10] and [11], two pilot design schemes based on cross-entropy optimization and stochastic approximation, respectively, are proposed to minimize the mean square error (MSE) using the channel data. In [12], a pilot allocation method based on genetic algorithm (GA) and shifting mechanism is proposed for multiple-input–multiple-output (MIMO) OFDM systems. In [13], a pilot design scheme for OFDM transmission over two-way relay networks is presented. However, it assumes the number of OFDM subcarriers to be prime.

In this paper, unlike the work in [10] and [11], we consider the pilot design based on the mutual incoherence property (MIP), which avoids acquiring of channel data. We first analyze the impact of different lengths of channel impulse response (CIR) and provide a sufficient condition that guarantees the pilot pattern generated from the CDS to be optimal. Then, we propose three pilot design schemes to obtain a near-optimal pilot pattern. The first two schemes are based on the stochastic search, namely, stochastic sequential search (SSS) and stochastic parallel search (SPS). The third scheme called iterative group shrinkage (IGS) removes rows in a group instead of removing a single row at each time. Considering the greedy manner of the IGS-based algorithm, a tree-based searching structure is applied to keep several best intermediate results rather than only the best result at each iteration. Finally, we extend our work to MIMO systems. Two schemes are proposed, including the sequential design and the joint design of the pilot

Manuscript received December 15, 2013; revised March 25, 2014; accepted June 11, 2014. Date of publication June 24, 2014; date of current version April 14, 2015. This work was supported in part by the National Natural Science Foundation of China under Grant 61302097 and Grant 61271018, by the National Science and Technology Major Project of China under Grant 2013ZX03003006-002, by the Ph.D. Programs Foundation of the Ministry of Education of China under Grant 20120092120014, and by the Research Project of Jiangsu Province under Grant BK20130019. The review of this paper was coordinated by Prof. Y. Su.

C. Qi, L. Wu, and Y. Huang are with the School of Information Science and Engineering, Southeast University, Nanjing 210096, China (e-mail: qch@seu.edu.cn; wuln@seu.edu.cn; huangym@seu.edu.cn).

G. Yue is with NEC Laboratories America, Inc., Princeton, NJ 08540 USA (e-mail: yueguosen@ieee.org).

A. Nallanathan is with the Center for Telecommunications Research, Department of Informatics, King's College London, London, U.K. (e-mail: nallanathan@ieee.org).

Color versions of one or more of the figures in this paper are available online at http://ieeexplore.ieee.org.

Digital Object Identifier 10.1109/TVT.2014.2331085

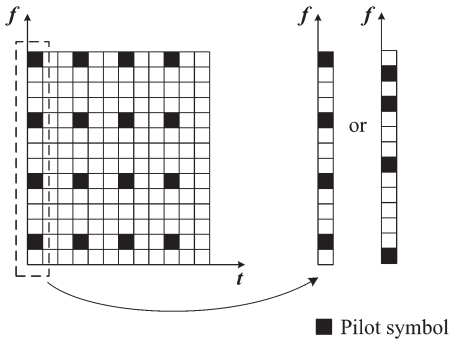

Fig. 1. Pilot pattern in OFDM systems.

patterns for multiple transmit antennas. Extensive numerical comparisons are conducted for the proposed SSS-, SPS-, and IGS-based pilot design schemes, as well as the extension schemes for MIMO systems. In particular, we compared the proposed SSS, SPS, and IGS schemes with the cross-entropy optimization [10], which has already shown to outperform GA [12] and particle swarm optimization (PSO).

The remainder of this paper is organized as follows. Section II formulates the OFDM pilot-assisted channel estimation as a sparse recovery problem. Section III presents a sufficient condition with respect to the CIR length for the pilot pattern generated from the CDS being optimal. The proposed pilot design schemes are presented in Section IV. Simulation results are provided in Section V. Finally, conclusions are provided in Section VI.

The notations used in this paper are defined as follows. Symbols for matrices (upper case) and vectors (lower case) are in boldface. $(\cdot)^T$, $(\cdot)^H$, $\mathrm{diag}\{\cdot\}$, $\boldsymbol{I}_L$, $\mathbb{C}^M$, $\mathbb{C}^{M\times N}$, $\mathbf{0}^M$, $\mathbf{0}^{M\times N}$, $\|\boldsymbol{a}\|_0$, $\mathcal{CN}$, $\setminus$, $\emptyset$, $\lceil\cdot\rceil$, and $\lfloor\cdot\rfloor$ denote the matrix transpose, conjugate transpose (Hermitian), the diagonal matrix, the identity matrix of size L, the set of complex vectors with dimension M, the set of $M\times N$ complex matrices, the zero vector with dimension M, the $M\times N$ zero matrix, the ℓ_0-norm that counts the nonzero number in $\boldsymbol{a}$, the complex Gaussian distribution, the set exclusion, the empty set, the ceiling function, and the floor function, respectively. For matrix $\boldsymbol{A}$, $A(i)$, $A[i]$, and $A[i,j]$ denote the ith column of $\boldsymbol{A}$, the ith row of $\boldsymbol{A}$, and the entry at the ith row and the jth column of $\boldsymbol{A}$, respectively. $a(i)$ denotes the ith entry of vector $\boldsymbol{a}$.

II. Problem Formulation

For pilot-assisted channel estimation in OFDM systems, we usually employ a comb-type pilot pattern on the time–frequency 2-D grids, as shown in the left portion of Fig. 1. Each column of the grids represents an OFDM symbol transmitted at a different time slot, and each row represents a subcarrier. Then, each subcarrier in an OFDM symbol forms the minimum resource unit, which is used to transmit either a pilot symbol or a data symbol. Once the subcarrier positions for the pilot symbols, marked in black in Fig. 1, are determined for some specified OFDM symbols, we use interpolations and channel tracking schemes, e.g., Kalman filtering, to obtain channel estimates for the other OFDM symbols. It is well known that, for the channel estimations based on least squares (LS) and minimum MSE methods, the optimal pilot pattern in OFDM systems is equally spaced pilot subcarriers [14]. However, for sparse channel estimation that uses sparse recovery algorithms, the optimal pilot pattern is still unknown. As shown in the right portion of Fig. 1, we present two examples of equally spaced pilots and non-equally spaced pilots. Motivated by showing whether the equally spaced pilot is the optimal or not, we consider the pilot design for sparse channel estimation by searching for the positions of pilot subcarriers, i.e., design a pilot pattern, in a specified OFDM symbol.

Consider an OFDM system with N subcarriers in each OFDM symbol, among which N_p pilot subcarriers indicated by $p_1, p_2, \ldots, p_{N_p}$ are used for frequency-domain pilot-assisted channel estimation. Without loss of generality, we assume that $1 \le p_1 < p_2 < \cdots < p_{N_p} \le N$. The corresponding transmit pilot symbols are denoted as $x(p_1), x(p_2), \ldots, x(p_{N_p})$. Let $h(1), h(2), \ldots, h(L)$ be the equivalent discrete CIR with the maximum multipath delay spread being L samples. The received signals on the pilot subcarriers can be written as

$$\begin{bmatrix} y(p_1) \\ y(p_2) \\ \vdots \\ y\left(p_{N_p}\right) \end{bmatrix} = \begin{bmatrix} x(p_1) & 0 & 0 & 0 \\ 0 & x(p_2) & 0 & 0 \\ 0 & 0 & \ddots & 0 \\ 0 & 0 & 0 & x\left(p_{N_p}\right) \end{bmatrix} \cdot \boldsymbol{F}_{N_p\times L} \cdot \begin{bmatrix} h(1) \\ h(2) \\ \vdots \\ h(L) \end{bmatrix} + \begin{bmatrix} \eta(1) \\ \eta(2) \\ \vdots \\ \eta(N_p) \end{bmatrix} \quad (1)$$

where $\eta(i) \sim \mathcal{CN}(0, \sigma_\eta^2)$, $i = 1, 2, \ldots, N_p$ is the independent and identically distributed (i.i.d.) additive white Gaussian noise, and $\boldsymbol{F}_{N_p\times L}$ is a discrete Fourier transform (DFT) submatrix, given by

$$\boldsymbol{F}_{N_p\times L} = \frac{1}{\sqrt{N}} \begin{bmatrix} 1 & \omega^{p_1} & \cdots & \omega^{p_1\cdot(L-1)} \\ 1 & \omega^{p_2} & \cdots & \omega^{p_2\cdot(L-1)} \\ \vdots & \vdots & \ddots & \vdots \\ 1 & \omega^{p_{N_p}} & \cdots & \omega^{p_{N_p}\cdot(L-1)} \end{bmatrix}$$

where $\omega = e^{-j2\pi/N}$. We denote

$$\begin{aligned} \boldsymbol{X} &\triangleq \mathrm{diag}\left\{x(p_1), x(p_2), \ldots, x\left(p_{N_p}\right)\right\} \\ \boldsymbol{y} &\triangleq \left[y(p_1), y(p_2), \ldots, y\left(p_{N_p}\right)\right]^T \\ \boldsymbol{h} &\triangleq \left[h(1), h(2), \ldots, h(L)\right]^T \\ \boldsymbol{\eta} &\triangleq \left[\eta(1), \eta(2), \ldots, \eta(N_p)\right]^T \sim \mathcal{CN}\left(\mathbf{0}, \sigma_\eta^2 \boldsymbol{I}_{N_p}\right). \end{aligned}$$

Furthermore, we let

$$\boldsymbol{A} \triangleq \boldsymbol{X}\boldsymbol{F}_{N_p\times L}. \quad (2)$$

Then, (1) can be rewritten as

$$\boldsymbol{y} = \boldsymbol{A}\boldsymbol{h} + \boldsymbol{\eta}. \quad (3)$$

If $\boldsymbol{A}$ has more rows than columns, i.e., $N_p \ge L$, then (3) is a standard LS problem with the estimated CIR given by

$$\hat{\boldsymbol{h}}_{\mathrm{LS}} = \left(\boldsymbol{A}^H\boldsymbol{A}\right)^{-1}\boldsymbol{A}^H\boldsymbol{y}. \quad (4)$$

However, we are more interested in the case of $N_p < L$ where we can save more pilots and therefore improve the data rate. In practice, since the sampling period is usually much smaller than the channel delay spread, most components of $\boldsymbol{h}$ are either zero or nearly zero, meaning that $\boldsymbol{h}$ is a sparse vector. With this *a priori* condition, we can use less pilots than the unknown channel coefficients, i.e., $N_p < L$, and apply CS algorithms to estimate $\boldsymbol{h}$. Many works have demonstrated that the CS algorithms outperform the LS method for channel estimation [15].

III. Analysis of Optimal Pilot Pattern: Cyclic Different Set

A. MIP for Pilot Design

Recent advances in CS show that, under noiseless condition, $\boldsymbol{h}$ can be reconstructed from the measurement $\boldsymbol{y}$ with a high probability when the dictionary matrix $\boldsymbol{A}$ satisfies the RIP [6]. However, there is no existing method having polynomial complexity to check whether a given matrix satisfies the RIP. Alternatively, according to [16], we can minimize the coherence of $\boldsymbol{A}$, which is known as the MIP. The MIP condition is stronger than RIP in that MIP implies the RIP but the converse is not true [17]. In addition, MIP is more intuitive and more practical than RIP. Therefore, in this paper, we consider the MIP as the pilot design rule.

For a given pilot pattern

$$\boldsymbol{p} = \left\{p_1, p_2, \ldots, p_{N_p}\right\}$$

where $1 \le p_1 < p_2 < \cdots < p_{N_p} \le N$, we define the coherence of $\boldsymbol{A}$ as the maximum absolute correlation between any two different columns of $\boldsymbol{A}$, i.e.,

$$\begin{aligned} g(\boldsymbol{p}) &\triangleq \max_{0\le m<n\le L-1} |\langle A(m), A(n)\rangle| \\ &= \max_{0\le m<n\le L-1} \left| \sum_{i=1}^{N_p} |x(p_i)|^2 \, \omega^{p_i(n-m)} \right| \end{aligned} \tag{5}$$

where $\langle A(m), A(n)\rangle$ denotes the inner product of $A(m)$ and $A(n)$, i.e., $\langle A(m), A(n)\rangle = A^H(m)A(n)$. The objective function for the pilot design is to minimize the coherence of $\boldsymbol{A}$, i.e.,

$$Q = \min_{\boldsymbol{p}} g(\boldsymbol{p}) \tag{6}$$

with respect to the pilot pattern $\boldsymbol{p}$. The solution of the optimization problem in (6), i.e., the optimal pilot pattern, is then given by

$$\boldsymbol{p}_{\text{opt}} = \arg\min_{\boldsymbol{p}} g(\boldsymbol{p}). \tag{7}$$

We assume equal transmit power among all OFDM pilot symbols, i.e.,

$$|x(p_1)|^2 = |x(p_2)|^2 = \cdots = \left|x\left(p_{N_p}\right)\right|^2 = E. \tag{8}$$

Let $c \triangleq n - m$. We then simplify (5) as

$$g(\boldsymbol{p}) = E \cdot \max_{1\le c\le L-1} \left| \sum_{i=1}^{N_p} \omega^{p_i c} \right|. \tag{9}$$

For some specific settings on the number of subcarriers and the number of pilot symbols in an OFDM symbol, the optimal pilot pattern can be generated from the CDS with the following definition.

Definition 1: Let N, K, and λ be positive integers where $K < N$. The CDS (N, K) is defined as a set of K distinct components, denoted as $\{\alpha_0, \alpha_1, \ldots, \alpha_{K-1}\}$ satisfying that any integer $Z\,(1 \le Z \le N-1)$ repeats exactly λ times in the set $\{\tau \triangleq \alpha_i - \alpha_l (\mathrm{mod}\, N) | 0 \le i \ne l \le K-1\}$, where

$$\lambda = \frac{K(K-1)}{N-1}. \tag{10}$$

For example, a CDS {1, 7, 9, 10, 12, 16, 26, 33, 34} with $N = 37$ and $K = 9$, which is denoted CDS(37, 9), satisfies that any integer $Z(1 \le Z \le 36)$ will occur and repeat exactly $\lambda = 2$ times in the set $\Theta \triangleq \{\tau \triangleq \alpha_i - \alpha_l (\mathrm{mod}\, 37) | 0 \le i \ne l \le 8\}$, where Θ has 72 entries.

A list of known CDS can be found in [18].

B. Sufficient Condition for CDS-Based Optimal Pilot Pattern

In [7], we have shown that, for an N-subcarrier OFDM system using N_p subcarriers as pilots, the pilot pattern according to the CDS (N, N_p) is optimal if the CDS (N, N_p) exists. However, later, we find that it is not always true, particularly for some small L. We now derive a sufficient condition for the optimal pilot pattern with the following theorem.

Theorem 1: With the sufficient condition

$$L \ge \left\lceil \frac{N}{2} \right\rceil \tag{11}$$

the pilot pattern generated from the CDS (N, N_p) is the optimal solution for (7), which achieves the Welch bound

$$\Gamma = E\sqrt{\frac{N_p(N-N_p)}{N-1}}. \tag{12}$$

Proof: See the Appendix. ■

We remark that the optimal pilot pattern for sparse channel estimation can be obtained from the CDS (N, N_p) if the channel length L is large enough. Nevertheless, the CDS only exists for some specific pair of (N, N_p). For most practical OFDM systems with N being a power of two, e.g., $N = 64, 256, 512,$ or 1024, the CDS does not exist. Even if the condition of N for the existence of the CDS is satisfied, various choices of N_p might be needed in practical systems. Moreover, we usually set the length of the cyclic prefix of OFDM to be $N/4$, which is much larger than the CIR length L, i.e.,

$$\frac{N}{4} \ge L \tag{13}$$

whereas the sufficient condition (11) is not satisfied. Therefore, it is important to explore practical schemes to design pilot pattern for any setting of (N, N_p) and any value of L.

IV. Pilot Design Schemes

Intuitively, by exhaustively searching over all possible pilot patterns, we can obtain the optimal pilot pattern with the minimum MIP. However, it is computationally prohibitive to search from all $\binom{N}{N_p}$ candidates when N and N_p are not very small. For example, if $N = 256$ and $N_p = 12$, we have $\binom{256}{12} = 1.27 \times 10^{21}$ different pilot patterns, which form a huge search space. Apparently, the exhaustive search is not a good option for future energy-efficient wireless systems [19] as it occupies a lot of computational resources that consume power and energy. Moreover, for those power-constrained mobile devices in cognitive radio networks [20], it is impractical to design the pilots using the exhaustive search.

We now propose three low-complexity practical schemes to obtain near-optimal pilot patterns for any given pair of (N, N_p) and for any value of L. The first two schemes are based on the stochastic search, which searches for the near-optimal pilot pattern with two loops of iterations. The third scheme, which is called IGS, forms the resulting pilot pattern in a reversed fashion by sequentially removing subcarriers from the subset of all available OFDM subcarriers until the number of the remaining OFDM subcarriers reaches the desired size of the pilot pattern.

A. Stochastic Search Schemes

The following two stochastic search schemes consist of two levels of loops. In the outer loop, we randomly generate pilot patterns as the initializations of the inner loop. In the inner loop, we iteratively update the resulting pilot pattern in a greedy manner. For the pilot update in the inner loop, we propose two alternatives, i.e., the sequential search and the parallel search. We now explain these two new stochastic schemes in detail as follows.

1) SSS: Given the maximum numbers of iterations for the outer and inner loops, i.e., M_1 and M_2, respectively, the SSS scheme is described as follows.

- In each iteration of the outer loop, we randomly generate a pilot pattern $\boldsymbol{p} \subset \mathcal{N} = \{1, \ldots, N\}$ as the initialization of the inner loop. In each iteration of the inner loop, we perform a sequential update of each entry of $\boldsymbol{p}$ according to the following step.

  — For $k = 1, \ldots, N_p$, given the latest $\boldsymbol{p}$ from the last iteration, we update the kth entry of $\boldsymbol{p}$ with the best one selected from $\mathcal{N} \setminus \{p(i) | i = 1, \ldots, N_p, i \neq k\}$, which results in the minimum MIP. Mathematically, the resulting pilot pattern $\hat{\boldsymbol{p}}$ with the update of the kth entry is given as

$$\hat{\boldsymbol{p}}_{\boldsymbol{p},k} = \arg \min_{\substack{\boldsymbol{p}^* \\ p^*(i)=p(i),\ i=1,2,\ldots,N_p,\ i\neq k \\ p^*(k)\in\mathcal{N}\setminus\{p(i),i=1,2,\ldots,N_p,i\neq k\}}} g(\boldsymbol{p}^*). \quad (14)$$

  After we obtain $\hat{\boldsymbol{p}}_{\boldsymbol{p},k}$ for given $\boldsymbol{p}$ and k, we let $\boldsymbol{p} = \hat{\boldsymbol{p}}_{\boldsymbol{p},k}$.

- For each initial pilot pattern in the outer loop, we obtain a corresponding optimized pilot pattern. With M_1 outer-loop iterations, we then obtain M_1 optimized results, from which we select the one with the minimum MIP as the final output.

The detailed algorithm for this scheme is presented in Algorithm 1. Note that for the inner loop, alternatively, we can continue updating $\boldsymbol{p}$ until it converges, meaning that it stops only when no update can be made after an inner-loop iteration completes. However, the computation time is difficult to control if the inner loop converges very slowly. Although this alternative approach may guarantee that the best result can be obtained after the inner-loop iterations, it may not be practical as the expected computational time is unknown. When we set a fixed number of inner-loop iterations as in Algorithm 1, it is possible that the pilot update converges earlier. To improve the efficiency of the algorithm, we then employ a simple *comparison and break* process as in steps 5–8 of Algorithm 1 for the early termination of the inner loop when it converges.

Algorithm 1: SSS-Based Pilot Design Algorithm

1: Initializations: Set M_1 and M_2. $\boldsymbol{D} \Leftarrow \boldsymbol{0}^{M_1 \times N_p}$. $\boldsymbol{r} \Leftarrow \boldsymbol{0}^{M_1}$.
2: **for** $l = 1, 2, \ldots, M_1$
3: randomly generate $\boldsymbol{p} \subset \mathcal{N}$. $\tilde{\boldsymbol{p}} \Leftarrow \boldsymbol{0}^{N_p}$.
4: **for** $n = 1, 2, \ldots, M_2$
5: **if** $\boldsymbol{p} = \tilde{\boldsymbol{p}}$
6: break.
7: **end if**
8: $\tilde{\boldsymbol{p}} \Leftarrow \boldsymbol{p}$.
9: **for** $k = 1, 2, \ldots, N_p$
10: Obtain $\hat{\boldsymbol{p}}_{\boldsymbol{p},k}$ according to (14). $\boldsymbol{p} \Leftarrow \hat{\boldsymbol{p}}_{\boldsymbol{p},k}$.
11: **end for** (k)
12: **end for** (n)
13: $D[l] \Leftarrow \boldsymbol{p}$. $r(l) \Leftarrow g(\boldsymbol{p})$.
14: **end for** (l)
15: $t = \arg\min_{i=1,2,\ldots,M_1} r(i)$.
16: output $D[t]$.

2) SPS: It is observed from Algorithm 1 that, in the inner loop, we sequentially update each entry of $\boldsymbol{p}$, meaning that we always use a newly updated $\boldsymbol{p}$ at the kth entry to obtain $\hat{\boldsymbol{p}}_{\boldsymbol{p},k+1}$ for the $(k+1)$-th entry. Since it is a greedy search algorithm, employing the sequential update for each entry may converge quickly to a local optimum. To be more conservative, we now present a parallel search scheme for the inner-loop update. Therefore, the only difference between this scheme and the SSS scheme is in the inner-loop iteration, which is presented as follows.

- In each iteration of the inner loop, we perform a parallel update of $\boldsymbol{p}$ according to the following steps.

  — For $k = 1, \ldots, N_p$, given the latest $\boldsymbol{p}$ from the previous inner-loop iteration, we obtain $\hat{\boldsymbol{p}}_{\boldsymbol{p},k}$ according to (14) for the kth entry. Note that unlike SSS, we do not immediately update $\boldsymbol{p}$ with $\hat{\boldsymbol{p}}_{\boldsymbol{p},k}$.

— We then obtain $\hat{\boldsymbol{p}}_{\boldsymbol{p},1}, \hat{\boldsymbol{p}}_{\boldsymbol{p},2}, \ldots, \hat{\boldsymbol{p}}_{\boldsymbol{p},N_p}$, each one corresponding to an entry update of $\boldsymbol{p}$. From them, we select the best update with the minimum MIP as the final update for this inner-loop iteration.

The detailed algorithm is described in Algorithm 2. We can see that in the SPS scheme, we try to find the best entry update in each inner-loop iteration. Since only one entry of $\boldsymbol{p}$ is updated in each inner-loop iteration, the convergence speed might be slower than that of SSS. However, the computation time can be reduced as the process can be implemented in parallel if parallel computing is supported by hardware.

Algorithm 2: SPS-Based Pilot Design Algorithm

1–8: The same as Algorithm 1.
9: $\boldsymbol{B} \Leftarrow \boldsymbol{0}^{N_p \times N_p}$. $\boldsymbol{v} \Leftarrow \boldsymbol{0}^{N_p}$.
10: **for** $k = 1, 2, \ldots, N_p$
11: Obtain $\hat{\boldsymbol{p}}_{\boldsymbol{p},k}$ according to (14).
12: Let $B[k] \Leftarrow \hat{\boldsymbol{p}}_{\boldsymbol{p},k}$ and $v(k) \Leftarrow g(\hat{\boldsymbol{p}}_{\boldsymbol{p},k})$.
13: **end for** (k)
14: $t = \arg\min_{i=1,2,\ldots,N_p} v(i)$. $\boldsymbol{p} \Leftarrow B[t]$.
15–19: The same as steps 12–16 of Algorithm 1.

B. IGS

It is easily seen that (9) is essentially a problem of finding the optimal row combinations from an N by L DFT submatrix denoted as

$$\boldsymbol{W} = \frac{1}{\sqrt{N}} \begin{bmatrix} 1 & 1 & \cdots & 1 \\ 1 & \omega & \cdots & \omega^{L-1} \\ \vdots & \vdots & \ddots & \vdots \\ 1 & \omega^{N-1} & \cdots & \omega^{(N-1)(L-1)} \end{bmatrix}.$$

Since the columns of $\boldsymbol{W}$ are orthonormal, the coherence of $\boldsymbol{W}$ is zero according to (5). Now, to choose the optimal N_p rows from $\boldsymbol{W}$ and form the corresponding pilot pattern, instead of exhaustively searching for the solution from all possible $\binom{N}{N_p}$ pilot patterns, we have proposed an efficient tree-based backward pilot generation scheme in [9], which iteratively removes rows from $\boldsymbol{W}$ one by one with the objective to minimize the coherence of the resulting matrix. With $N - N_p$ iterations, the indices of the remaining N_p rows form a near-optimal pilot pattern. Moreover, in each iteration, instead of keeping only one best resulting submatrix, we keep N_t best candidates, which becomes an N_t-best tree-based search algorithm.

In this paper, to further improve the performance, we propose a more generalized tree-based scheme called IGS. With this scheme, in each iteration, we jointly select and remove N_r rows from the latest updated submatrix so that the submatrix with the remaining rows has the smallest coherence. Before describing the scheme, we first extend the definition of MIP function $g(\boldsymbol{p})$ in (5) and define

$$g_{\boldsymbol{W}}(\boldsymbol{q}) \triangleq \max_{0 \le m < n \le L-1} |\langle W_{\boldsymbol{q}}(m), W_{\boldsymbol{q}}(n) \rangle| \tag{15}$$

where $\boldsymbol{q} \subset \mathcal{N} = \{1, \ldots, N\}$ can be a subset with any size smaller than N, $\boldsymbol{W}_{\boldsymbol{q}}$ is a submatrix formed by the selected rows of $\boldsymbol{W}$ with row indices given by $\boldsymbol{q}$, and $W_{\boldsymbol{q}}(n)$ denotes the nth column of $\boldsymbol{W}_{\boldsymbol{q}}$. Given the predetermined N_r and N_t, the IGS scheme is described as follows.

- With the initial $\mathcal{N}$, we exhaustively search a subset $\Phi \subset \mathcal{N}$ with $\|\Phi\|_0 = N_r$, and for each obtained Φ, we calculate the objective $g_{\boldsymbol{W}}(\boldsymbol{q})$ according to (15) where $\boldsymbol{q} = \mathcal{N} \setminus \Phi$. From all of $\binom{N}{N_r}$ obtained subsets, we choose N_t best subsets, i.e., $\Phi_1, \Phi_2, \ldots, \Phi_{N_t}$, with N_t smallest objective. Define $\tilde{N} = N - N_r$ and $\tilde{\mathcal{N}}_i = \mathcal{N} \setminus \Phi_i$, $i = 1, \ldots, N_t$. In other words, we construct a tree whose top level includes N_t parent nodes representing N_t best subsets $\Phi_1, \Phi_2, \ldots, \Phi_{N_t}$.
- Iteratively select N_r rows from the remaining $\tilde{N}$ rows and update $\tilde{\mathcal{N}}_i$, $i = 1, \ldots, N_t$. From the perspective of the tree structure, we understand it as iteratively generating N_t^2 leaf nodes from the N_t parent nodes, and then selecting N_t best leaf nodes as parents nodes for the next iteration. Eventually, we select a best branch stringed by the surviving nodes and then remove the branch from $\mathcal{N}$ and output the remaining row indices as the designed pilot pattern. The iterative steps can be described as follows.

  — For each $\tilde{\mathcal{N}}_i$, $i = 1, \ldots, N_t$, from the last iteration, we exhaustively search over all subsets $\Phi \subset \tilde{\mathcal{N}}_i$ to find the N_t best results. Considering that if N_r does not divide $(N - N_p)$, in the last iteration, we remove $\tilde{N} - N_p$ rows instead of removing N_r rows; the size of Φ is set as $l \triangleq \|\Phi\|_0 = \min\{N_r, \tilde{N} - N_p\}$. For each obtained Φ, we calculate the objective $g_{\boldsymbol{W}}(\boldsymbol{q})$ according to (15) where $\boldsymbol{q} = \tilde{\mathcal{N}}_i \setminus \Phi$. From all of $\binom{\tilde{N}}{l}$ obtained subsets, we find N_t best subsets, i.e., $\Phi_{i1}, \Phi_{i2}, \ldots, \Phi_{iN_t}$, with N_t smallest objective. Then we update $\tilde{N} = \tilde{N} - l$.
  — If it is the last iteration, i.e., $\tilde{N} \le N_p$, we find the best result Φ_{i^*,k^*} from $\{\Phi_{i,k}, i = 1, \ldots, N_t, k = 1, \ldots, N_t\}$ obtaining the final result $\boldsymbol{p}^* = \tilde{\mathcal{N}}_{i^*} \setminus \Phi_{i^*,k^*}$. Then we terminate the procedure and output $\boldsymbol{p}^*$.
  — If $\tilde{N} > N_p$, from $\{\Phi_{i,k}, i = 1, \ldots, N_t, k = 1, \ldots, N_t\}$ with N_t^2 entries, we select N_t best entries Φ_{i_s,k_s}, $s = 1, \ldots, N_t$. We obtain $\tilde{\mathcal{N}}'_s = \tilde{\mathcal{N}}_{i_s} \setminus \Phi_{i_s,k_s}$, $s = 1, \ldots, N_t$. Then we update $\tilde{\mathcal{N}}_s = \tilde{\mathcal{N}}'_s$, $s = 1, \ldots, N_t$.

We can see that when $N_r = N - N_p$, it is equivalent to the exhaustive search of $\binom{N}{N_p}$. If $N_r = 1$, it becomes the pilot design scheme in [9]. Usually, N_r is supposed to be small, e.g., $N_r = 2$, so that $\binom{N}{N_r}$ is computationally inexpensive. Including the initial search of N_t best subsets, the total number

of iterations for IGS is then $\lceil (N - N_p)/N_r \rceil$. The detailed procedures are presented in Algorithm 3.

Algorithm 3: IGS-Based Pilot Design Algorithm

Set N_t and N_r. $\mathcal{N} \Leftarrow \{1, \ldots, N\}$.
Exhaustively search from all subsets $\Phi \subset \mathcal{N}$ with $\|\Phi\|_0 = N_r$ to find N_t best subsets $\Phi_1, \Phi_2, \ldots, \Phi_{N_t}$.
$\tilde{N} \Leftarrow N - N_r$. $\tilde{\mathcal{N}}_i \Leftarrow \mathcal{N} \setminus \Phi_i$, $i = 1, \ldots, N_t$.
while $\tilde{N} > N_p$ **do**
  Let $l = \min\{N_r, \tilde{N} - N_p\}$.
  for $i = 1, 2, \ldots, N_t$
    Exhaustively search from all subsets $\Phi \subset \tilde{\mathcal{N}}_i$ with $\|\Phi\|_0 = l$. Find N_t best subsets $\Phi_{i1}, \Phi_{i2}, \ldots, \Phi_{iN_t}$.
  end for (i)
  $\tilde{N} \Leftarrow \tilde{N} - l$.
  if $\tilde{N} \leq N_p$
    Among N_t^2 results $\{\Phi_{i,k}, i = 1, \ldots, N_t, k = 1, \ldots, N_t\}$, find the best one as Φ_{i^*,k^*}.
    Obtain $\boldsymbol{p}^* = \tilde{\mathcal{N}}_{i^*} \setminus \Phi_{i^*,k^*}$. Break.
  else
    Among N_t^2 results $\{\Phi_{i,k}, i = 1, \ldots, N_t, k = 1, \ldots, N_t\}$, find N_t best Φ_{i_s,k_s}, $s = 1, \ldots, N_t$.
    Obtain $\tilde{\mathcal{N}}'_s = \tilde{\mathcal{N}}_{i_s} \setminus \Phi_{i_s,k_s}$, $s = 1, \ldots, N_t$.
    Update $\tilde{\mathcal{N}}_s = \tilde{\mathcal{N}}'_s$, $s = 1, \ldots, N_t$.
  end if
end while
Output the final result $\boldsymbol{p}^*$.

C. Extension to MIMO Systems

The proposed stochastic search schemes, including SSS and SPS, can be readily extended to MIMO systems with N_u transmit antennas and N_v receive antennas. We assume that $N_u \leq \lfloor N/N_p \rfloor$. Let

$$\boldsymbol{p}^{(i)} = \left\{ p_1^{(i)}, p_2^{(i)}, \ldots, p_{N_p}^{(i)} \right\}, \quad i = 1, \ldots, N_u$$

denote the pilot pattern at the ith transmit antenna. Suppose that $\boldsymbol{p}^{(i)} \cap \boldsymbol{p}^{(l)} = \emptyset$ for $i \neq l$, i.e., the pilot patterns for different transmit antennas are orthogonal so that the receiver can perform individual sparse channel estimation for the channel from each transmit antenna.

A straightforward way to extend the proposed pilot design scheme for MIMO system is to design $\{\boldsymbol{p}^{(i)}\}_{i=1}^{N_u}$ sequentially. Such an extension, which is called the Extension Scheme 1, is described as follows.

1) Initialize $\mathcal{N}^{(1)} = \mathcal{N}$, and obtain $\boldsymbol{p}^{(1)}$ using SSS or SPS.
2) For $i = 2, \ldots, N_u$, update $\mathcal{N}^{(i)} = \mathcal{N}^{(i-1)} \setminus \boldsymbol{p}^{(i-1)}$, and obtain $\boldsymbol{p}^{(i)}$ using SSS or SPS from subset $\mathcal{N}^{(i)}$.
3) Output $\{\boldsymbol{p}^{(i)}\}_{i=1}^{N_u}$.

Nevertheless, this scheme may result in unfairness among N_u transmit antennas as $\mathcal{N}^{(N_u)} \subset \cdots \subset \mathcal{N}^{(1)}$. For the first transmit antenna, the pilot pattern $\boldsymbol{p}^{(1)}$ is selected from N OFDM subcarriers, whereas for the last transmit antenna, the pilot pattern $\boldsymbol{p}^{(N_u)}$ is selected from remaining only $N - (N_u - 1)N_p$ subcarriers. Therefore, the performance degradation may occur for the transmit antenna with the last designed pilot patterns, particularly for large N_u. In the time-division duplexing (TDD) systems, the channel state information at transmitter required for the downlink beamforming is obtained by estimating the uplink channel at the base station using the channel reciprocity [21]. Therefore, the number of pilot patterns to be transmitted in TDD systems might be very large due to the limited time–frequency resource available in the uplink channel and the large number of mobile stations, e.g., in massive MIMO systems [22], [23]. A quite common scenario in practical is that, during the pilot training phase of the uplink transmission, an entire OFDM symbol is used for pilot transmissions, meaning that all OFDM subcarriers in this OFDM symbol are allocated for pilot symbols and thus divided into a number of orthogonal pilot patterns assigned to different users. Therefore, ensuring the fairness among the pilot patterns of different users is particularly important when designing multiple orthogonal pilot patterns.

We now propose another extension scheme for MIMO systems, termed as Extension Scheme 2, which jointly designs $\{\boldsymbol{p}^{(i)}\}_{i=1}^{N_u}$ to achieve certain fairness. Without loss of generality, we consider designing the N_u orthogonal pilot patterns for N_u transmit antennas. Denote

$$\boldsymbol{w} = \Bigg\{ \underbrace{p_1^{(1)}, p_2^{(1)}, \ldots, p_{N_p}^{(1)}}_{\boldsymbol{p}^{(1)}}, \underbrace{p_1^{(2)}, p_2^{(2)}, \ldots, p_{N_p}^{(2)}}_{\boldsymbol{p}^{(2)}}, \ldots, \underbrace{p_1^{(N_u)}, p_2^{(N_u)}, \ldots, p_{N_p}^{(N_u)}}_{\boldsymbol{p}^{(N_u)}} \Bigg\}.$$

Note that in the definition of $\boldsymbol{w}$ stated previously, there is an implicit order defined for $\boldsymbol{w}$, i.e., $\boldsymbol{p}^{(i)} = \{w((i-1)N_p + 1), \ldots, w(iN_p)\}$, meaning that the first N_p entries of the set $\boldsymbol{w}$ form the first pilot pattern $\boldsymbol{p}^{(1)}$, the second N_p entries of the set $\boldsymbol{w}$ form the second pilot pattern $\boldsymbol{p}^{(2)}$, and so on. However, the order for the entries within a particular $\boldsymbol{p}^{(i)}$ does not matter. We then define the objective function for joint pilot design as the weighted sum coherence of N_u pilot patterns given by

$$\zeta(\boldsymbol{w}) = \sum_{i=1}^{N_u} b_i g\left(\boldsymbol{p}^{(i)}\right) \tag{16}$$

where b_i is the weight of the ith transmit antenna. The joint design is then to find the optimal $\boldsymbol{w}$, which minimizes this objective function, i.e., the weighted sum coherence, as

$$\boldsymbol{w} = \arg \min_{\boldsymbol{w}^* \subset \mathcal{N}} \zeta(\boldsymbol{w}^*). \tag{17}$$

We consider the extension of the SSS scheme for MIMO systems as Extension Scheme 2, which consists of one outer loop and two inner loops. The outer loop is similar to the loop in the SSS scheme in which we generate a random $\boldsymbol{w} \subset \mathcal{N}$ with $\|\boldsymbol{w}\|_0 = N_p N_u$. In the first inner loop, we iteratively apply SSS to find an optimal $\boldsymbol{w}$. Then, in the second inner loop,

given the resulting $\boldsymbol{w}$ from the first inner loop, we apply a so-called permutation step to obtain the best combinations of $\boldsymbol{p}^{(i)}$, $i = 1, \ldots, N_u$, i.e., the best order of $\boldsymbol{w}$ with the minimum weighted sum coherence $\zeta(\boldsymbol{w})$. Given M_1 and M_2 as the number of outer-loop iterations and the number of inner-loop iterations, respectively, Extension Scheme 2 using SSS is then summarized as follows.

- In each outer-loop iteration, we randomly generate a $\boldsymbol{w} \subset \mathcal{N} = \{1, \ldots, N\}$ with $\|\boldsymbol{w}\|_0 = N_p N_u$ as the initial N_u pilot patterns for N_u different transmit antennas.
- *SSS step*: We iteratively perform the following step.
  - For $k = 1, \ldots, N_p N_u$, given the latest $\boldsymbol{w}$ from the last iteration, we update $\boldsymbol{w}$ by replacing the kth entry with the best entry selected from $\mathcal{N} \setminus \{w[i] | i = 1, \ldots, N_p N_u, i \neq k\}$, which results in the minimum weighted sum coherence. Mathematically, the resulting $\hat{\boldsymbol{w}}$ with the update of the kth entry is given as

$$\hat{\boldsymbol{w}}_{\boldsymbol{w},k} = \arg \min_{\substack{\boldsymbol{w}^* \\ w^*[i]=w[i],\ i=1,2,\ldots,N_pN_u,\ i\neq k \\ w^*[k]\in\mathcal{N}\setminus\{w[i],i=1,2,\ldots,N_pN_u,i\neq k\}}} \zeta(\boldsymbol{w}^*). \quad (18)$$

- *Permutation step*: We iteratively perform the following step.
  - For $k = 1, \ldots, N_p N_u$, given the latest $\boldsymbol{w}$ from the last iteration, we exchange the entry $w[k]$ with one entry in $\{w[i] | i = 1, 2, \ldots, N_p N_u, \lceil i/N_p \rceil \neq \lceil k/N_p \rceil\}$ and keep all the other entries of $\boldsymbol{w}$ fixed, obtaining a new $\boldsymbol{w}^*$ and the corresponding $\zeta(\boldsymbol{w}^*)$. From all $(N_u - 1)N_p$ exchanges, we select one that results in the smallest weighted sum coherence to update $\boldsymbol{w}$. Mathematically, the resulting $\breve{\boldsymbol{w}}$ after the permutation at the kth entry is given as

$$\breve{\boldsymbol{w}}_{\boldsymbol{w},k} = \arg \min_{\substack{\boldsymbol{w}^* \\ w^*[k]=w[i],\ w^*[i]=w[k],\ i=1,\ldots,N_pN_u,\ \lceil \frac{i}{N_p} \rceil \neq \lceil \frac{k}{N_p} \rceil \\ w^*[k']=w[k'],\ k'=1,2,\ldots,N_pN_u,\ k'\neq k,k'\neq i}} \zeta(\boldsymbol{w}^*). \quad (19)$$

- For each initial $\boldsymbol{w}$ in the outer loop, we obtain a corresponding optimized result of $\boldsymbol{w}$. With M_1 outer-loop iterations, we then obtain M_1 optimized results, from which we select the minimum one as the final output.

The detailed algorithm is described in Algorithm 4, where the SSS steps are indicated by steps 4–11 and the permutation steps are indicated by steps 12–19. Similarly, we can come up with the SPS-based extension scheme for the MIMO joint pilot design algorithm.

Algorithm 4: SSS-Based MIMO Joint Pilot Design Algorithm (Extension Scheme 2)

1: Set M_1 and M_2. $M_3 \Leftarrow N_p N_u$. $\boldsymbol{D} \Leftarrow \mathbf{0}^{M_1 \times M_3}$. $\boldsymbol{r} \Leftarrow \mathbf{0}^{M_1}$.
2: **for** $l = 1, 2, \ldots, M_1$
3: randomly generate $\boldsymbol{w} \subset \mathcal{N}$. $\tilde{\boldsymbol{w}} \Leftarrow \mathbf{0}^{M_3}$.
4: Set $n = 0$.
5: **do**
6: $\tilde{\boldsymbol{w}} \Leftarrow \boldsymbol{w}$.
7: **for** $k = 1, 2, \ldots, M_3$
8: Obtain $\hat{\boldsymbol{w}}_{\boldsymbol{w},k}$ according to (18). $\boldsymbol{w} \Leftarrow \hat{\boldsymbol{w}}_{\boldsymbol{w},k}$.
9: **end for** (k)
10: $n \Leftarrow n + 1$.
11: **while** $(\boldsymbol{w} \neq \tilde{\boldsymbol{w}}$ **and** $n < M_2)$
12: Set $n = 0$.
13: **do**
14: $\tilde{\boldsymbol{w}} \Leftarrow \boldsymbol{w}$.
15: **for** $k = 1, 2, \ldots, M_3$
16: Obtain $\breve{\boldsymbol{w}}_{\boldsymbol{w},k}$ according to (19). $\boldsymbol{w} \Leftarrow \breve{\boldsymbol{w}}_{\boldsymbol{w},k}$.
17: **end for** (k)
18: $n \Leftarrow n + 1$.
19: **while** $(\boldsymbol{w} \neq \tilde{\boldsymbol{w}}$ **and** $n < M_2)$
20: $D[l] \Leftarrow \boldsymbol{w}$. $r(l) \Leftarrow \zeta(\boldsymbol{w})$.
21: **end for** (l)
22: $t = \arg\min_{i=1,2,\ldots,M_1} r(i)$.
23: output $D[t]$.

TABLE I
SUFFICIENT CONDITION (11) IS VERIFIED

N	N_p	L_{Th}	$\lceil \frac{N}{2} \rceil$	Welch bound
31	6	11	16	2.2361
23	11	12	12	2.4495
21	5	8	11	2
19	9	10	10	2.2361
15	7	8	8	2
13	4	6	7	1.7321
11	5	6	6	1.7321
7	3	4	4	1.4142

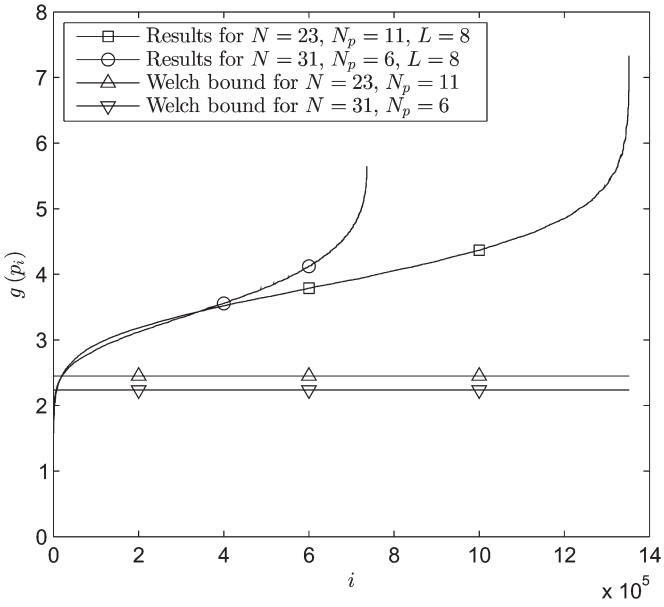

Fig. 2. Results of $g(\boldsymbol{p})$ in the ascending order over exhaustively generated $\boldsymbol{p}$ for $(N = 31, N_p = 6)$ and $(N = 23, N_p = 11)$ with $L = 8$. Both cases do not satisfy the sufficient condition in (11).

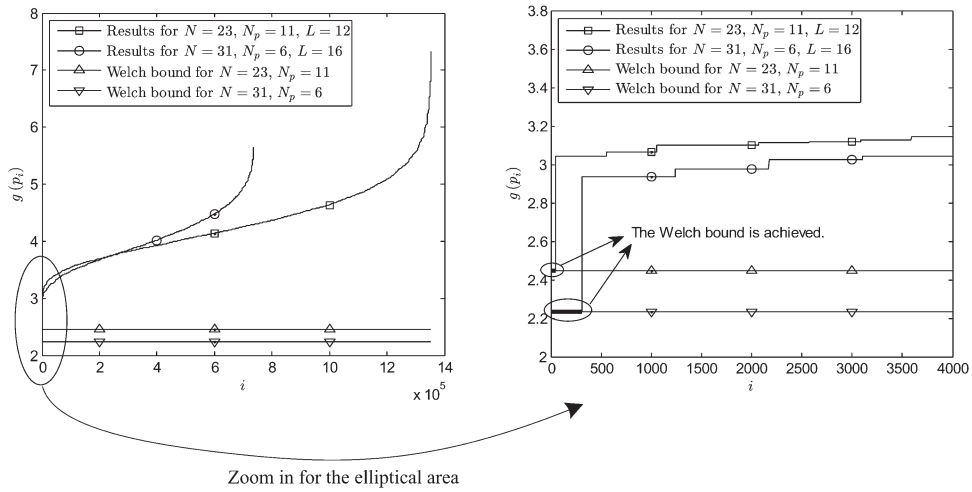

Fig. 3. Results of $g(\boldsymbol{p})$ in the increasing order over exhaustively generated $\boldsymbol{p}$ for $(N = 31, N_p = 6)$ with $L = 16$ and $(N = 23, N_p = 11)$ with $L = 12$. Both cases satisfy the sufficient condition in (11).

V. Simulation Results

A. CDS-Based Optimal Pilot Design

We first validate the sufficient condition of CDS-based optimal pilot pattern given in (11). Without loss of generality, we set $E = 1$. In Table I, we list some settings of (N, N_p) pair where CDS exists from [18]. For each setting of (N, N_p), we obtain the optimal pilot pattern for various L settings by the exhaustive search. We find that if L is greater than some threshold L_{Th}, as presented in Table I, the resulting optimal solution achieves the Welch bound. When $L < L_{\mathrm{Th}}$, the optimal pilot pattern can achieve a smaller MIP than the Welch bound, indicating that the CDS-based pilot pattern is no longer optimal. Although for some settings of (N, N_p), e.g., (31, 6), L_{Th} can be smaller than $\lceil N/2 \rceil$ for the CDS-based pilot pattern being optimal, (11) is the sufficient condition that generally applies for any given (N, N_p) if the CDS exists.

We choose the first two settings of (N, N_p) as (31, 6) and (23, 11) from Table I and exhaustively generate all $\binom{31}{6}$ and $\binom{23}{11}$ pilot patterns $\boldsymbol{p}$, respectively. We then evaluate $g(\boldsymbol{p})$ in (5) for every pilot pattern and for various values of L. The results of $g(\boldsymbol{p})$ sorted in the ascending order are shown in Fig. 2 with $L = 8$ for both settings and in Fig. 3 with $L = 16$ for (31, 6) and $L = 12$ for (23, 11). The Welch bounds, i.e., 2.2361 for (31, 6) and 2.4495 for (23, 11), are also presented in both figures for comparisons. Since $L = 8$ does not satisfy the sufficient condition (11) for both (31, 6) and (23, 11), it is shown in Fig. 2 that there do exist some pilot patterns with smaller $g(\boldsymbol{p})$ than the Welch bound. However, as shown in Fig. 3, when both settings satisfy the sufficient condition, the Welch bound is the lower bound that can be achieved by the optimal pattern for the corresponding (N, N_p) setting. To clearly show the pilot patterns that achieve the Welch bound, the elliptical area in the left portion of Fig. 3 is zoomed in and presented in the right portion of Fig. 3. We find that 310 and 46, or equivalently 0.042% and 0.0034%, pilot patterns are able to achieve the Welch bounds for (31, 6) and (23, 11), respectively. Moreover, it is noticed that there is a steep drop of $g(\boldsymbol{p})$ to the Welch bound in the vicinity area of the optimal pilot patterns for both curves, indicating that there is a large gap between the performance achieved by the optimal pilot pattern and that by the best suboptimal pilot pattern. It is also the reason why there seems a gap between the optimal performance and the Welch bounds in the elliptical area in the left portion of Fig. 3.

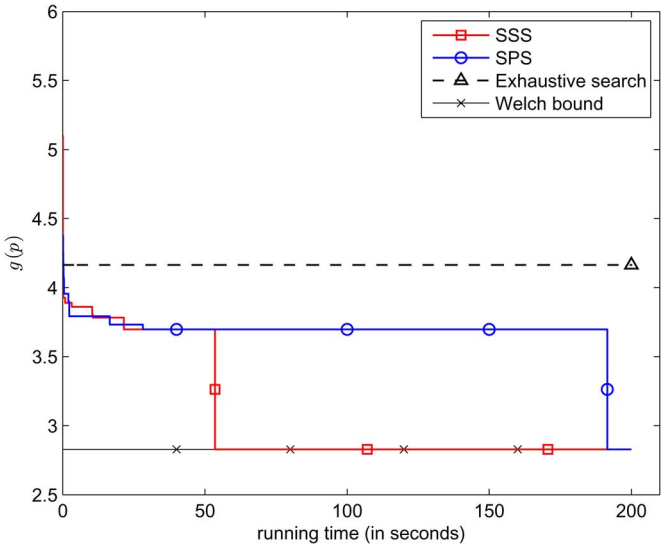

Fig. 4. Comparisons of SSS, SPS, the exhaustive search, and the Welch bound for $N = 73$ and $N_p = 9$.

B. Performance of Pilot Design Schemes for Single Pilot Pattern

We first consider the case of $N = 73$, $N_p = 9$, and $L = 37$, which satisfies the sufficient condition in (11) for the optimal pilot pattern with the Welch bound 2.8284. For this case, it is almost impossible to perform the exhaustive search to obtain the optimal solution due to the large candidate set of $\binom{73}{9}$ pilot patterns. Therefore, we only apply the low-complexity design schemes to obtain a near-optimal pilot pattern, namely, the proposed SSS and SPS schemes. Since both schemes are iterative methods, we present the updating histories of $g(\boldsymbol{p})$ in

TABLE II
PERFORMANCE OF THE IGS PILOT DESIGN SCHEME WITH VARIOUS N_r SETTINGS FOR $N = 73$, $N_p = 9$, $N_t = 2$, AND $L = 37$

N_r	Q	Running time
1	4.8150	1.76
2	4.3776	22.52
3	4.1252	274.98
4	3.9742	2824.45

Fig. 4. The Welch bound and the results of the exhaustive search are also provided for comparisons. For the exhaustive search, we generate the pilot pattern randomly, and the best result obtained during a predetermined maximum running time is the final output of the exhaustive search.[1] For fair comparisons, the simulations are performed using exactly the same computer hardware and software.[2] The updating histories of $g(\boldsymbol{p})$ are presented as a function of the running time, and the maximum running time is set as 200 s for all schemes. In Fig. 4, we observe that both SSS and SPS can find the optimal pilot pattern that achieves the Welch bound, indicating that the proposed stochastic search schemes are more efficient than the exhaustive search. Moreover, we find that SSS converges much faster than SPS as the former achieves the Welch bound much earlier than the latter.

We now evaluate the performance of the IGS scheme, which is implemented according to Algorithm 3. Here, we only present the final result, which is the designed pilot pattern with the performance $Q = g(\boldsymbol{p})$ at the last step. The intermediate results are not very meaningful as the resulting subsets at intermediate steps are not the desired pilot patterns with size N_p. The results of Q and the running time are provided in Table II with various N_r settings for $N = 73$, $N_p = 9$, $N_t = 2$, and $L = 37$. If $N_r = 1$, the IGS scheme is essentially the scheme proposed in [9]. It is shown in Table II that as N_r increases, the resulting Q reduces and the running time increases, indicating that this scheme performs better for larger N_r but with increasing complexity. Compared with the SSS and SPS schemes using the same parameters shown in Fig. 4, the IGS scheme results in larger Q with more running time. Therefore, although the proposed IGS scheme improves the performance over the scheme in [9], the proposed SSS and SPS schemes are more efficient.

We now consider practical OFDM systems in which the number of subcarriers is usually a power of two and the CDS does not exist. We evaluate the performance of the proposed pilot design schemes for the case of $N = 256$ and $N_p = 16$. We set $L = 60$ as indicated in (13).

We first present the results of the IGS scheme with various N_t and N_r settings in Table III. The designed pilot patterns $\boldsymbol{p}_d$ are provided in the last column. It is seen that for this case, the setting of $N_t = 4$ and $N_r = 2$ achieves the best performance with the resulting $Q = g(\boldsymbol{p}_d)$ smaller than that of $N_t = 16$ and $N_r = 1$, indicating that increasing N_r is more effective than increasing N_t, but at the cost of the complexity.

TABLE III
PERFORMANCE OF THE IGS PILOT DESIGN SCHEME WITH VARIOUS N_t AND N_r SETTINGS FOR THE OFDM SYSTEMS WITH $N = 256$, $N_p = 16$, AND $L = 60$

N_t	N_r	Q	Running time	$\boldsymbol{p}_d$
2	1	5.5543	41	6, 26, 30, 33, 53, 59, 76, 79, 84, 87, 95, 171, 185, 201, 214, 251
2	2	4.9795	1893	20, 44, 52, 64, 96, 112, 116, 140, 152, 172, 188, 196, 200, 204, 208, 236
4	1	5.1493	80	6, 10, 14, 66, 98, 138, 142, 146, 162, 178, 210, 218, 230, 242, 246, 254
4	2	4.8462	3641	3, 14, 59, 62, 94, 97, 105, 116, 123, 131, 144, 184, 194, 209, 212, 216
12	1	5.0209	240	24, 32, 36, 40, 52, 56, 68, 80, 92, 105, 125, 152, 156, 200, 208, 216
16	1	4.9193	340	10, 14, 66, 90, 94, 142, 146, 162, 178, 206, 210, 218, 230, 242, 250, 254

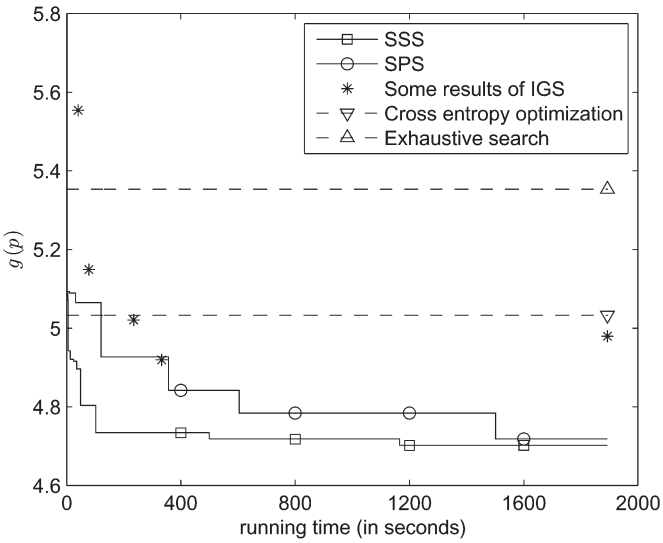

Fig. 5. Comparisons of different schemes to design the pilot pattern.

Fig. 5 shows the updating histories of $g(\boldsymbol{p})$ as a function of running time for the proposed SSS and SPS, as well as some results of the IGS scheme from Table III and marked as points corresponding to the resulting Q and the running time needed. The results of cross-entropy optimization [10] and the exhaustive search are also given for comparisons. The stopping time for all these schemes is set as 1893 s, which is the time required by the IGS scheme with $N_t = 2$ and $N_r = 2$. The obtained $Q = g(\boldsymbol{p}_d)$ with the corresponding designed pilot pattern $\boldsymbol{p}_d$ is provided in Table IV. It is shown in Fig. 5 that all the proposed methods, including the SSS, SPS, and IGS schemes, perform much better than the cross-entropy optimization and the exhaustive search in terms of both Q and the convergence rate. Since cross-entropy optimization has already shown to outperform GA and PSO [25], it is demonstrated that SSS, SPS, and IGS perform better than the GA used in [12]. It is also observed that the SSS and SPS schemes outperform the IGS

[1]Generally, the exhaustive search is a brute-force method that exhaustively examines all possibilities. However, since the generation of all $\binom{73}{9} = 9.7 \times 10^{10}$ candidates is almost impossible, we define the exhaustive search with consistency with most works in the literature [24].

[2]The simulations are performed using MATLAB v7.12 (R2011a) on a laptop equipped with an Intel Core 2 Duo CPU at 2.5 GHz and 3 GB of memory. Although all presented schemes are iterative methods, we use the same running time (in seconds) instead of the same number of iterations for comparisons as the complexity in each iteration is different for different schemes.

TABLE IV
PERFORMANCE COMPARISONS OF PILOT DESIGN SCHEMES FOR $N = 256$, $N_p = 16$, AND $L = 60$

Type	Q	p_d
SSS	4.7021	8, 40, 48, 52, 72, 82, 99, 142, 145, 154, 158, 161, 183, 209, 212, 230
SPS	4.7184	2, 24, 77, 80, 93, 109, 123, 141, 144, 148, 152, 160, 181, 204, 245, 254
IGS	4.9795	20, 44, 52, 64, 96, 112, 116, 140, 152, 172, 188, 196, 200, 204, 208, 236
Cross entropy optimization	5.0328	42, 58, 70, 78, 83, 91, 94, 109 150, 179, 201, 210, 235, 250, 253, 256
Exhaustive search	5.3535	35, 38, 45, 47, 49, 71, 74, 79, 99, 115, 147, 156, 174, 194, 213, 240

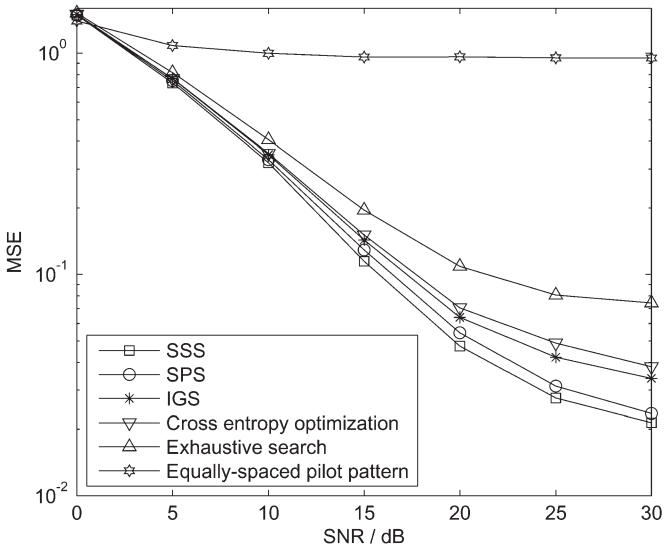

Fig. 6. MSE performance comparisons of channel estimation for different pilot design schemes.

scheme. Although both SSS and SPS result in similar Q values, the former converges much faster than the latter.

We next compare the channel estimation performance using the designed pilot patterns given in Table IV. The sparse multipath channel is modeled with $L = 60$ taps, where $S = 6$ dominant nonzero channel taps are randomly placed among L taps. The channel gain of each path is i.i.d. complex Gaussian distributed with unit variance, i.e., $\mathcal{CN}(0, 1)$. We use this model for 2000 sparse channel implementations in the simulations. The popular OMP algorithm is employed for the sparse recovery. The equally spaced pilot pattern is also treated as it proves to be the best for traditional channel estimation methods. The MSE performance for channel estimation and the bit-error-rate (BER) performance for data detection are presented in Figs. 6 and 7, respectively. We observe that the pilot obtained from SSS performs slightly better than that from SPS, but both outperform that obtained from the cross entropy and the exhaustive search. The pilot pattern obtained from IGS also shows some improvement over the ones from the existing two schemes. About 10-dB performance gain in SNR is achieved at BER $= 0.04$ using the proposed schemes instead of the exhaustive search. With channel encoding and decoding, BER around 0.01 can be completely removed in practical systems.

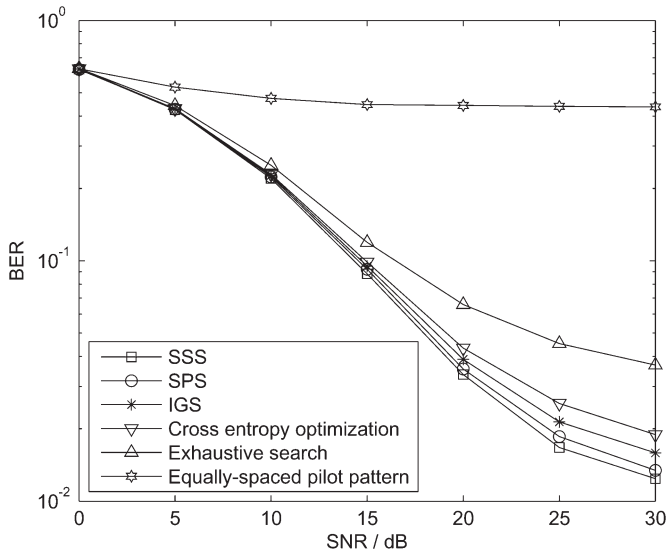

Fig. 7. BER performance comparisons of channel estimation for different pilot design schemes.

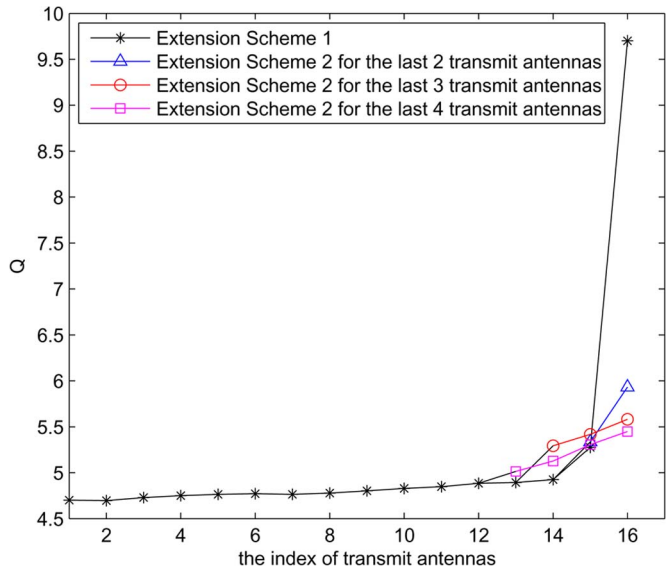

Fig. 8. Pilot design for MIMO systems using different extension schemes.

Moreover, we find that there is no benefit in using the equally spaced pilot pattern for sparse channel estimation since it is not optimized according to (7).

C. Performance of Pilot Design Schemes for Multiple Pilot Patterns

We now evaluate the performance of the proposed extension schemes for MIMO systems with N_u transmit antennas. Again, we consider the case of $N = 256$, $N_p = 16$, and set $N_u = N/N_p = 16$. This is the full pilot loading case in which an entire OFDM symbol is allocated for pilot transmissions along different transmit antennas. The performance of the proposed Extension Scheme 1 and Extension Scheme 2 is shown in Fig. 8 with some detailed results provided in Table V. It is noted that, to reduce the complexity, we combine two extension schemes, first applying Extension Scheme 1 to sequentially obtain the

TABLE V
COMPARISONS OF TWO PILOT DESIGN SCHEMES FOR MIMO SYSTEMS

Type of the schemes and parameters	Objective $Q = g(\boldsymbol{p}^{(m)})$ of the mth transmit antenna				Average of the last n transmit antennas		
	$m = 13$	$m = 14$	$m = 15$	$m = 16$	$n = 2$	$n = 3$	$n = 4$
Extension Scheme 1	4.894	4.924	5.276	9.701	7.489	6.634	6.199
Extension Scheme 2 for $m = 15, 16$			5.336	5.932	5.634		
Extension Scheme 2 for $m = 14, 15, 16$		5.293	5.418	5.582		5.431	
Extension Scheme 2 for $m = 13, 14, 15, 16$	5.013	5.128	5.306	5.448			5.224

pilot patterns for most antennas and then applying Extension Scheme 2 to jointly design the pilot patterns for the rest of the antennas. It is shown in Fig. 8 that the results of Extension Scheme 1 are fairly good for transmit antennas 1–14, indicating that this scheme is quite efficient to design most pilot patterns. However, the performance of the pilot patterns for the last two antennas is much worse than that of others. This drastic change is due to the greedy manner of the sequential design. Therefore, it is necessary to jointly design the pilot patterns for the last few antennas using Extension Scheme 2 to minimize the weighted sum coherence. For simplicity, we consider equal weights, i.e., $b_1 = b_2 = \cdots = b_{16} = 1/16$. We consider joint design of the last two, three, or four transmit antennas. As shown in Fig. 8, the performance of the last antenna is significantly improved, with slight performance degradation on the other antennas involved in the joint design. In Table V, we see that the performance of the $m = 16$th transmit antenna improves with Q reduced by 38.9%, 42.5%, and 43.8% over that from Extension Scheme 1 when we employ Extension Scheme 2 for the last $n = 2$, $n = 3$, and $n = 4$ transmit antennas, respectively. In terms of the weighted sum coherence, 24.8%, 18.1%, and 15.7% improvement over that employing only Extension Scheme 1 can be achieved when applying Extension Scheme 2 for the joint design of the pilot patterns for the last $n = 2$, $n = 3$, and $n = 4$ transmit antennas, respectively.

VI. CONCLUSION

In this paper, we have considered the MIP-based pilot design schemes for sparse channel estimation in OFDM systems. With respect to the CIR length, we have derived a sufficient condition to guarantee that the pilot pattern generated from the CDS is optimal. We have proposed three pilot design schemes, including SSS, SPS, and IGS, to obtain a near-optimal pilot pattern. We have also extended to MIMO systems to design multiple orthogonal pilot patterns and have proposed two design schemes termed as Extension Scheme 1 and Extension Scheme 2. Simulation results have demonstrated the effectiveness of the proposed schemes and have shown that the proposed schemes converge much faster than the cross-entropy optimization and the exhaustive search schemes. Moreover, the proposed SSS and SPS schemes outperform the IGS scheme in terms of channel estimation performance. For MIMO systems, Extension Scheme 2 performs better than Extension Scheme 1. However, the combination of two extension schemes achieves the best performance and complexity tradeoff.

APPENDIX
PROOF OF THEOREM 1

We define

$$f(c) \triangleq \left| \sum_{i=1}^{N_p} \omega^{p_i c} \right|^2 = \sum_{i=1}^{N_p} \sum_{l=1}^{N_p} \omega^{c(p_i - p_l)}, \quad 1 \le c \le L-1. \tag{20}$$

Our objective is equivalently to minimize $\max_{1 \le c \le L-1} f(c)$ according to (6) and (9). Let $d = (p_i - p_l) \bmod N$, $1 \le i \ne l \le N_p$. Then, for all possible $d \in \{1, 2, \ldots, N-1\}$, we denote a_d as the number of occurrences of d. We then have the following two constraints on a_d, which are given by

$$\sum_{d=1}^{N-1} a_d = N_p(N_p - 1), \quad a_d \ge 0 \tag{21}$$

$$a_d = a_{N-d}, \quad d = 1, 2, \ldots, \left\lfloor \frac{N}{2} \right\rfloor. \tag{22}$$

The reason for (21) is that when computing d, each pair of (p_i, p_l) in order, $i \ne l$, will occur only once. Therefore, the total number of occurrences of all possible d, which is denoted as $\sum_{d=1}^{N-1} a_d$, is equal to the number of permutations of (p_i, p_l), which is $N_p(N_p - 1)$.

We then have

$$f(c) = N_p + \sum_{d=1}^{N-1} a_d \cdot \omega^{cd}, \quad 1 \le c \le L-1. \tag{23}$$

Since $\omega^d \ne 1$ for $d = 1, \ldots, N-1$, we obtain

$$\sum_{c=1}^{L-1} f(c) = N_p(L-1) + \sum_{d=1}^{N-1} a_d \frac{\omega^d - \omega^{Ld}}{1 - \omega^d}. \tag{24}$$

Further using the inequality

$$\max_{1 \le c \le L-1} f(c) \ge \frac{1}{L-1} \sum_{c=1}^{L-1} f(c) \tag{25}$$

we have

$$\max_{1 \le c \le L-1} f(c) \ge N_p + \frac{1}{L-1} \sum_{d=1}^{N-1} a_d \frac{\omega^d - \omega^{Ld}}{1 - \omega^d}. \tag{26}$$

The equality of (26) holds only with

$$f(1)=f(2)=\cdots=f(L-1)\triangleq\beta=N_p+\frac{1}{L-1}\sum_{d=1}^{N-1}a_d\frac{\omega^d-\omega^{Ld}}{1-\omega^d}. \tag{27}$$

We denote

$$\boldsymbol{a}=[0,a_1,a_2,\ldots,a_{N-1}]^T$$
$$\boldsymbol{z}=\left[N_p(N_p-1),\underbrace{\kappa,\kappa,\ldots,\kappa}_{L-1}\right]^T$$

where we define

$$\kappa\triangleq\beta-N_p.$$

Then, from (21) and (23), we have

$$\boldsymbol{z}=\boldsymbol{F}_L\cdot\boldsymbol{a} \tag{28}$$

where $\boldsymbol{F}_L$ is an L by N DFT submatrix formed by the first L rows of the standard N by N DFT matrix.

If $L=N$, which is a special case discussed in [26], we can straightforwardly solve the N unknowns from the N equations in (28) obtaining

$$a_1=a_2=\cdots=a_{N-1}=\frac{N_p(N_p-1)}{N-1} \tag{29}$$

$$\beta=\frac{N_p(N-N_p)}{N-1}. \tag{30}$$

It is known that the CDS satisfies the Welch bound [26]

$$\Gamma=E\sqrt{\beta}=E\sqrt{\frac{N_p(N-N_p)}{N-1}} \tag{31}$$

and therefore minimizes the coherence of $\boldsymbol{A}$. Therefore, in this case, the pilot pattern generated from the CDS is optimal.

Now, we consider the more general cases when $L<N$. For (28), we have L equations and N unknown variables, including $N-1$ unknown components $a_1,a_2,\ldots,a_{N-1}$ of $\boldsymbol{a}$ and the unknown κ of $\boldsymbol{z}$. Notice that there are $\lfloor N/2\rfloor$ implicit equations given in (22). Hence, we have actually $L+\lfloor N/2\rfloor$ equations for the N unknown variables, which means that $L+\lfloor N/2\rfloor\geq N$, or equally $L\geq\lceil N/2\rceil$, is sufficiently required. This completes the proof.

REFERENCES

[1] W. U. Bajwa, J. Haupt, A. M. Sayeed, and R. Nowak, "Compressed channel sensing: A new approach to estimating sparse multipath channels," *Proc. IEEE*, vol. 98, no. 6, pp. 1058–1076, Jun. 2010.

[2] C. Qi, X. Wang, and L. Wu, "Underwater acoustic channel estimation based on sparse recovery algorithms," *IET Signal Process.*, vol. 5, no. 8, pp. 739–747, Dec. 2011.

[3] D. Hu, X. Wang, and L. He, "A new sparse channel estimation and tracking method for time-varying OFDM systems," *IEEE Trans. Veh. Technol.*, vol. 62, no. 9, pp. 4648–4653, Nov. 2013.

[4] Y. Barbotin and M. Vetterli, "Fast and robust parametric estimation of jointly sparse channels," *IEEE J. Emerging Sel. Topics Circuits Syst.*, vol. 2, no. 3, pp. 402–412, Sep. 2012.

[5] F. Wan, W.-P. Zhu, and M. N. S. Swamy, "Semiblind sparse channel estimation for MIMO-OFDM systems," *IEEE Trans. Veh. Technol.*, vol. 60, no. 6, pp. 2569–2582, Jul. 2011.

[6] E. J. Candes and T. Tao, "Decoding by linear programming," *IEEE Trans. Inf. Theory*, vol. 51, no. 12, pp. 4203–4215, Dec. 2005.

[7] C. Qi and L. Wu, "A study of deterministic pilot allocation for sparse channel estimation in OFDM systems," *IEEE Commmun. Lett.*, vol. 16, no. 5, pp. 742–744, May 2012.

[8] P. Pakrooh, A. Amini, and F. Marvasti, "OFDM pilot allocation for sparse channel estimation," *EURASIP J. Adv. Signal Process.*, vol. 59, no. 1, pp. 1–9, Mar. 2012.

[9] C. Qi and L. Wu, "Tree-based backward pilot generation for sparse channel estimation," *Electron. Lett.*, vol. 48, no. 9, pp. 501–503, Apr. 2012.

[10] J.-C. Chen, C.-K. Wen, and P. Ting, "An efficient pilot design scheme for sparse channel estimation in OFDM systems," *IEEE Commmun. Lett.*, vol. 17, no. 7, pp. 1352–1355, Jul. 2013.

[11] C. Qi and L. Wu, "Optimized pilot placement for sparse channel estimation in OFDM systems," *IEEE Signal Process. Lett.*, vol. 18, no. 12, pp. 749–752, Dec. 2011.

[12] X. He, R. Song, and W.-P. Zhu, "Pilot allocation for sparse channel estimation in MIMO-OFDM systems," *IEEE Trans. Circuits Syst. II, Exp. Briefs*, vol. 60, no. 9, pp. 612–616, Sep. 2013.

[13] P. Cheng *et al.*, "Sparse channel estimation for OFDM transmission over two-way relay networks," in *Proc. IEEE ICC*, Ottawa, ON, Canada, Jun. 2012, pp. 3948–3953.

[14] L. Tong, B. M. Sadler, and M. Dong, "Pilot-assisted wireless transmissions: General model, design criteria, signal processing," *IEEE Signal Process. Mag.*, vol. 21, no. 6, pp. 12–26, Nov. 2004.

[15] C. R. Berger, Z. Wang, J. Huang, and S. Zhou, "Application of compressive sensing to sparse channel estimation," *IEEE Commmun. Mag.*, vol. 48, no. 11, pp. 164–174, Nov. 2010.

[16] D. Donoho and X. Huo, "Uncertainty principles and ideal atomic decomposition," *IEEE Trans. Inf. Theory*, vol. 47, no. 7, pp. 2845–2862, Nov. 2001.

[17] T. Cai and L. Wang, "Orthogonal matching pursuit for sparse signal recovery with noise," *IEEE Trans. Inf. Theory*, vol. 57, no. 7, pp. 4680–4688, Jul. 2011.

[18] La Jolla Cyclic Difference Set Repository. [Online]. Available: http://www.ccrwest.org/diffsets/ds_list.pdf

[19] D. Feng *et al.*, "A survey of energy-efficient wireless communications," *IEEE Commun. Surveys Tuts.*, vol. 15, no. 1, pp. 167–178, Feb. 2013.

[20] C. Qi, G. Yue, L. Wu, and A. Nallanathan, "Pilot design for sparse channel estimation in OFDM-based cognitive radio systems," *IEEE Trans. Veh. Technol.*, vol. 63, no. 2, pp. 982–987, Feb. 2014.

[21] Y. Huang *et al.*, "Distributed multicell beamforming with limited intercell coordination," *IEEE Trans. Signal Process.*, vol. 59, no. 2, pp. 728–738, Feb. 2011.

[22] B. Gopalakrishnan and N. Jindal, "An analysis of pilot contamination on multi-user MIMO cellular systems with many antennas," in *Proc. IEEE 12th Int. Workshop SPAWC*, San Francisco, CA, USA, Jun. 2011, pp. 381–385.

[23] D. Gesbert *et al.*, "Multi-cell MIMO cooperative networks: A new look at interference," *IEEE J. Sel. Areas Commun.*, vol. 28, no. 9, pp. 1380–1408, Dec. 2010.

[24] I. Berenguer, X. Wang, and V. Krishnamurthy, "Adaptive MIMO antenna selection via discrete stochastic optimization," *IEEE Trans. Signal Process.*, vol. 53, no. 11, pp. 4315–4329, Nov. 2005.

[25] J.-C. Chen and C.-K. Wen, "A novel cognitive radio adaptation for wireless multicarrier systems," *IEEE Commun. Lett.*, vol. 14, no. 7, pp. 629–631, Jul. 2010.

[26] P. Xia, S. Zhou, and G. B. Giannakis, "Achieving the Welch bound with difference sets," *IEEE Trans. Inf. Theory*, vol. 51, no. 5, pp. 1900–1907, May 2005.

Chenhao Qi (S'06–M'10) received the B.S. and Ph.D. degrees in signal processing from Southeast University, Nanjing, China, in 2004 and 2010, respectively.

From 2008 to 2010, he visited the Department of Electrical Engineering, Columbia University, New York, NY, USA. Since 2010, he has been with the faculty of the School of Information Science and Engineering, Southeast University, where he is currently an Associate Professor. His research interests include sparse signal processing and wireless communications.

Dr. Qi serves as a Reviewer and a Technical Program Committee Member for several international conferences.

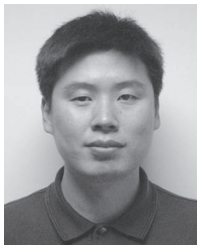

Guosen Yue (S'03–M'04–SM'09) received the B.S. degree in physics and the M.S. degree in electrical engineering from Nanjing University, Nanjing, China, in 1994 and 1997, respectively, and the Ph.D. degree in electrical engineering from Texas A&M University, College Station, TX, USA, in 2004.

Since August 2004, he has been a Research Staff with the Mobile Communications and Networking Research Department, NEC Laboratories America, Inc., Princeton, NJ, USA, conducting research for broadband wireless systems and mobile networks. His research interests are in the general areas of wireless communications and signal processing.

Dr. Yue served as the Symposium Co-chair for the IEEE International Conference on Communications in 2010; the Track Co-chair for the IEEE International Conference on Computing, Communication, and Networking in 2008; and a Steering Committee Member for the IEEE Radio and Wireless Symposium in 2009. He serves as an Associate Editor for the IEEE TRANSACTIONS ON WIRELESS COMMUNICATIONS. He has served as the Associate Editor for *Research Letters in Communications* and the Guest Editor for the European Association for Signal Processing (EURASIP) *Journal of Wireless Communications and Networking* special issue on interference management and Elsevier *PHYCOM* special issue on signal processing and coding.

Lenan Wu received the M.S. degree in electronic communication systems from Nanjing University of Aeronautics and Astronautics, Nanjing, China, in 1987 and the Ph.D. degree in signal and information processing from Southeast University, Nanjing, in 1997.

Since 1997, he has been with the faculty of the School of Information Science and Engineering, Southeast University, where he is currently a Professor and the Director of the Multimedia Technical Research Institute. He is the author or coauthor of more than 400 technical papers and 11 textbooks. He is the holder of 30 Chinese patents and one international patent. His research interests include multimedia information systems and communication signal processing.

Yongming Huang (M'10) received the B.S. and M.S. degrees from Nanjing University, Nanjing, China, in 2000 and 2003, respectively, and the Ph.D. degree in electrical engineering from Southeast University, Nanjing, in 2007.

Since March 2007, he has been with the faculty of the School of Information Science and Engineering, Southeast University. During 2008–2009, he was visiting the Signal Processing Laboratory, School of Electrical Engineering, Royal Institute of Technology (KTH), Stockholm, Sweden. His current research interests include space–time wireless communications, cooperative wireless communications, energy-efficient wireless communications, and optimization theory.

Dr. Huang serves as an Associate Editor for the IEEE TRANSACTIONS ON SIGNAL PROCESSING, the European Association for Signal Processing (EURASIP) *Journal on Advances in Signal Processing*, and the EURASIP *Journal on Wireless Communications and Networking*.

Arumugam Nallanathan (S'97–M'00–SM'05) received the B.Sc. degree with honors from the University of Peradeniya, Sri-Lanka, in 1991, the CPGS degree from the University of Cambridge, Cambridge, U.K., in 1994, and the Ph.D. degree from the University of Hong Kong, Hong Kong, in 2000, all in electrical engineering.

He is currently a Professor of wireless communications with the Department of Informatics, King's College London (University of London), London, U.K. He served as the Head of Graduate Studies of the School of Natural and Mathematical Sciences, King's College London, during 2011–2012. He was an Assistant Professor with the Department of Electrical and Computer Engineering, National University of Singapore, Singapore, from August 2000 to December 2007. His research interests include 5G technologies, millimeter-wave communications, cognitive radio, and relay networks. In these areas, he coauthored more than 200 papers.

Prof. Nallanathan currently serves as the Chair of the Signal Processing and Communication Electronics Technical Committee of the IEEE Communications Society. He served as the Technical Program Co-Chair (MAC track) for the IEEE Wireless Communications and Networking Conference in 2014; a Co-Chair for the IEEE Global Communications Conference (GLOBECOM) in 2013 (Communications Theory Symposium), the IEEE International Conference on Communications (ICC) in 2012 (Signal Processing for Communications Symposium), the IEEE GLOBECOM in 2011 (Signal Processing for Communications Symposium), the IEEE ICC in 2009 (Wireless Communications Symposium), and the IEEE GLOBECOM in 2008 (Signal Processing for Communications Symposium); the Technical Program Co-Chair for the IEEE ICUWB in 2011; and the General Track Chair for the IEEE Vehicular Technology Conference in 2008. He is a Distinguished Lecturer of the IEEE Vehicular Technology Society. He is an Editor of the IEEE TRANSACTIONS ON COMMUNICATIONS and the IEEE TRANSACTIONS ON VEHICULAR TECHNOLOGY. He was an Editor of the IEEE TRANSACTIONS ON WIRELESS COMMUNICATIONS (2006–2011), the IEEE WIRELESS COMMUNICATIONS LETTERS, and the IEEE SIGNAL PROCESSING LETTERS and a Guest Editor of the European Association for Signal Processing (EURASIP) *Journal on Wireless Communications and Networks* special issue on UWB communication systems-technology and applications (2006). He received the IEEE Communications Society Signal Processing and Communications Electronics (SPCE) Outstanding Service Award 2012. He coreceived the Best Paper Award presented at the 2007 IEEE International Conference on Ultra-Wideband (ICUWB 2007).